

An experimental study on the post-cracking behaviour of Hybrid Industrial/Recycled Steel Fibre-Reinforced Concrete

Enzo Martinelli^{a,*}, Antonio Caggiano^{b,c}, Hernan Xargay^b

^a *Department of Civil Engineering, University of Salerno, Italy.*

^b *LMNI, FIUBA, Laboratory of Materials and Structures, Faculty of Engineering, University of Buenos Aires, Argentina.*

^c *National Scientific and Technical Research Council (CONICET), Argentina.*

* *Corresponding author, Tel.: +39 089 964098; fax: +39 089 964045; e-mail: e.martinelli@unisa.it (E. Martinelli) acaggiano@fi.uba.ar (A. Caggiano), hxargay@fi.uba.ar (H. Xargay),*

Abstract

This paper investigates the mechanical behaviour of FRC made with both industrial and recycled steel fibres recovered from waste tyres. Specimens of various mixtures, characterised by the same volume fraction of fibres, but different proportions of industrial and recycled reinforcement were tested both in compression and four-point bending. The results highlighted no significant influence of fibres emerged in terms of compressive strength, whereas a significant decay in the post-cracking behaviour was observed in specimens with higher fractions of recycled fibres. However, a significant enhancement of the bending response was generally observed with the respect to the case of plain concrete, even in case of specimens reinforced by recycled fibres only.

Keywords: Waste Tyres; Concrete; FRC; Recycled Steel Fibre; Hybrid; Post-cracking behaviour.

1. Introduction

In recent years the disposal of exhaust tyres has emerged as a big issue in waste management [1] and the increasing amount of these waste actually constitutes a serious threat for both the environment and the human health

5 [2]. Moreover, based on the “Council Directive 1999/31/EC” of the European
6 Commission on the Landfill of Waste, as of 2003 post-consumer “whole tyres”
7 could no longer be landfilled and, since July 2006, such regulations must be
8 applied to either “whole” or “shredded” tyres [3].

9 Therefore, there are strong motivations for recycling such waste mate-
10 rials that can easily be turned into a **eco-friendly** source of secondary raw
11 materials [4]. In fact, recycling processes of waste tyres mainly consist of
12 separating the internal steel reinforcement from the rubber covering. Hence,
13 rubber scraps and short steel **fibres** are generally obtained by these pro-
14 cesses and can be utilised in several valuable applications. Particularly, they
15 can be used as concrete components in partial-to-total replacement of the
16 ordinary constituents (**e.g., natural aggregates and industrial fibres, respec-**
17 **tively**). On the one hand, rubber scraps find an interesting field of application
18 as a partial replacement of ordinary stone aggregates for obtaining the so-
19 called “rubberised concrete”, which is characterised by enhanced dumping
20 and toughness properties [5, 6]; on the other hand, recycled **fibres** can be
21 used in substitution of the industrial ones commonly employed for producing
22 **Fibre-Reinforced Cementitious Composites (FRCCs)** [7, 8].

23 As a matter of fact, adding a small fraction (usually in the order of 0.5-
24 1.0 % in volume) of short **fibres** during mixing, results in enhancing **the**
25 **toughness in the post-cracking response** of cementitious materials as they
26 have a bridging effect across the opening cracks and, then, a positive influence
27 on their propagation [9].

28 However, **fibres** employed in FRCC need to have good mechanical prop-
29 erties, be easy to spread in concrete mixtures and durable when embedded
30 into cementitious matrices [10]. Many types of **fibres** (i.e., made of steel,
31 glass, natural cellulose, carbon, nylon, polypropylene, etc.) have been used
32 in FRCC and are widely available for commercial applications [11]. In fact, a
33 total of 60 million tonnes of these kinds of **fibres** are currently employed every
34 year around the world, and, then, their production requires a huge amount
35 of raw materials [12]. Therefore, Recycled Steel **Fibres (RSFs)** obtained from
36 waste tyres could contribute to reducing **this** demand. Particularly, they can
37 directly be utilised as a dispersed reinforcement in concrete to obtain a ma-
38 terial which could be designated as Recycled Steel-FRC. In this regard, some
39 pioneer researches already demonstrated the feasibility of these applications
40 [13, 14, 15].

41 Innovative researches on FRC also address the possible use of mixed **fi-**
42 **bres** made of different material and/or geometry which can, in principle,

43 play a synergistic role in enhancing the post-cracking response of structural
44 members. These kinds of fibre-reinforced cement-based composites are often
45 referred to as Hybrid FRC (HyFRC). Experimental tests aimed at investi-
46 gating the HyFRC failure behaviour in direct tension have been performed,
47 among others, by Sorelli et al. [16] and Park et al.[17]. The mechanical
48 behaviour measured by means of indirect tensile tests have been proposed
49 on Hy-Polypropylene FRC [18], Hy-Steel FRC [19] or combining several fi-
50 bres: i.e., Carbon/Steel/Polypropylene FRC [20] or Steel/Palm/Synthetic
51 FRC [21]. Other relevant contributions regarding HyFRC with lightweight
52 aggregates [22], high-volume coarse fly ash [23], HyFRC exposed to high tem-
53 peratures [24] or self compacting HyFRC [25] have also been proposed within
54 the scientific community.

55 This paper deals with the mechanical behaviour of FRC with both indus-
56 trial and RSFs obtained from waste tyres, as mentioned above. In fact, it is
57 mainly based on the results of an experimental campaign carried out at the
58 Laboratory of Materials testing and Structures (LMS) of the University of
59 Salerno (Italy). Starting from a FRC mixture with 0.5 % (in volume), **that is**
60 **to say 40 kg/m³**, of Industrial Steel **Fibres** (ISFs), three more mixtures were
61 prepared by replacing 25 %, 50 % and 100 % **in weight** of such **fibres** with
62 an equal amount of RSFs. Therefore, the mechanical behaviour of conven-
63 tional Steel **Fibre**-Reinforced Concrete (SFRC) was observed in comparison
64 with the one of both Hybrid Industrial/Recycled Steel **Fibre**-Reinforced Con-
65 crete (HIRSFRC) and Recycled Steel **Fibre**-Reinforced Concrete (RSFRC).
66 The experimental campaign was mainly aimed at observing the key aspects
67 of both cubic samples tested in compression and notched beam specimens
68 tested in four-point bending (4PB) according to UNI-11039-1 [26] and UNI-
69 11039-2 [27].

70 **Investigating the mechanical response of the aforementioned HIRSFRC**
71 **and, particularly, quantifying the effect of replacing industrial fibres with an**
72 **equal amount (in weight) of recycled ones is the main original aspect of this**
73 **paper. In the authors' best knowledge no experimental investigation was car-**
74 **ried out so far for comparing the mechanical response of FRC characterised**
75 **by an invariant volume fraction of fibres and variable proportion of industrial**
76 **and recycled ones; in fact, the results currently available in the literature are**
77 **always referred to the two "extreme" cases of FRC with either industrial**
78 **or recycled fibres. Therefore, the results presented in this paper might be**
79 **useful to readers interested in calibrating theoretical models and numerical**
80 **procedures intended at simulating the effect induced by partially replacing**

81 ISFs with RSFs.

82 Finally, the paper is organised as follows. Sect. 2 preliminarily describes
83 the key geometric properties of the RSF employed in this research, whereas
84 the complete definition of the adopted “materials and methods” is reported
85 in Sect. 3. Then, Sect. 4 reports the results of both compression and bending
86 tests and Sect. 5 proposes a systematic analysis based upon well-established
87 standard parameters describing the post-cracking response of FRC. In con-
88 clusion, the key findings of the present study are outlined in Sect. 6, along
89 with some comments about their conceptual significance and insights on the
90 future developments of this research.

91 2. Recycled steel fibres from waste tyres

92 The recycled steel fibres (Fig. 1) employed in this study were supplied
93 by a company whose main business consists in collecting and recycling ex-
94 hausted tyres. Particularly, 15 kg of RSFs were received at LMS and sampled
95 to obtain a comprehensive description of their variable geometry, being the
96 mechanical characterisation not covered in this paper and specifically ad-
97 dressed in dedicated experimental campaign which is currently going on.

98 First of all, fibres were cleaned and separated from some thicker pieces of
99 steel, which were not clearly suited for being used as a spread reinforcement
100 of FRC. Fig. 2 reports two Scanning Electron Microscope (SEM) images
101 revealing that residual rubber impurities, no wider than 20-25 μm , were still
102 attached to the fibre surface.

103 Then, a detailed geometric characterisation was carried out on a bunch
104 of about 2000 RSFs, randomly sampled from the available amount of RSFs.
105 The diameter (d_f) was measured by means of a micrometer: particularly,
106 three measures were taken (i.e., at the two ends and at the mid-point) and
107 an average value was determined for each fibre. According to such measure-
108 ments, the average fibre diameter was ranging between 0.11 and 1.64 mm:
109 Fig. 3 highlights its apparently multimodal distribution (probably due to
110 the mixing of different types of tyres in the recycling process) characterised
111 by a mean value of 0.27 mm. However, more than one third (35.7 %) of the
112 sampled fibres exhibited an average diameter between 0.22 and 0.24 mm.

113 The geometric characterisation of RSFs was completed by determining
114 the fibre length l_f which was conventionally defined, according to the CNR-
115 204/2006 [28] specifications, as the distance between the outer ends of a
116 fibre. Fig. 4 shows the frequency distribution of measured fibre lengths: in

117 this case a unimodal distribution was observed (probably resulting from the
118 unified cutting underwent during the recycling process): the mean value was
119 about 12 mm and almost one half of measured fibre lengths (47.1 % of the
120 total amount) was found ranging between 9-15 mm, whereas the 10 %, 50 %
121 and 90 % percentiles were of 18, 24 and 37 mm, respectively.

122 Furthermore, the total “developed length” l_d [28] was also measured for
123 the same sample of fibres: Fig. 5 shows the resulting unimodal frequency
124 distribution of l_d . Moreover the l_f/l_d ratio was also determined for describing
125 the shape of the same fibres (Fig. 6): values of this ratio closer to unit
126 corresponds to fairly straight fibres, whereas the lower this ratio the more
127 curled and twisted the fibre.

128 Finally, the aspect ratio (l_f/d_f) of fibres was analysed, as it is a key pa-
129 rameter which controls their mechanical performance in FRC. Fig. 7 high-
130 lights a unimodal distribution of the aspect ratio, with a mean value of about
131 47 and more than one half (57 %) of fibres exhibited a value within the range
132 30-60: in fact these values are rather close to the aspect ratios commonly
133 characterising industrial steel fibres [11].

134 3. Experimental campaign

135 The results reported in this section were obtained from an experimental
136 programme developed at the Laboratory of Materials testing and Structures
137 (LMS) of the University of Salerno (Italy). The experimental tests were
138 performed according to UNI-11039-1 [26] for definitions, classification and
139 designation and UNI-11039-2 [27] for the test method.

140 3.1. Materials

141 The FRCs specimens tested in this study were prepared by adopting a
142 unique mixture for the concrete matrix which was also employed for preparing
143 the plain concrete specimens considered as a reference (labelled as REF). This
144 mixture was designed for a target 28 days mean cubic compressive strength of
145 40 MPa and prepared by using crushed limestone aggregates with a maximum
146 aggregate size of 20 mm according to EN-12620 [29] and UNI-11039-1 [26], a
147 constant cement content of 320 kg /m³ and a free water to-cement-ratio w/c
148 of 0.51. Table 1 describes the mixture composition: coarse natural aggregates
149 with grain size ranging between 2 and 10 mm were denoted as $N1$, whereas
150 $N2$ corresponds to grain size from 10 to 20 mm. Moreover, fine aggregates
151 (namely “sand”) were characterised by a maximum equivalent size equal to 2

152 mm. Table 2 reports the specific weight and water absorption capacity of the
153 aforementioned aggregates and sand. The aggregate grading of the reference
154 concrete is represented in Fig. 8 in comparison with the well-known Fuller
155 grain size distribution.

156 Wirand Fibres type FS7 Fig. 9, already considered by the authors in a
157 previous experimental campaign [30] and generally referred to as “Industrial
158 Steel Fibres” (ISFs) in the following, were considered in this study along with
159 the RSFs already described in details in Sect. 2 (Fig. 1). The key geometric
160 and mechanical properties of ISFs are listed in the following [31]: $l_f = 33$
161 mm (fibre length), $d_f = 0.55$ mm (fibre diameter), $AR = 60$ (aspect ratio),
162 number of fibres per kg = 16100, $f_t > 1200$ MPa (failure strength in tension)
163 and $\varepsilon_u \leq 2\%$ (ultimate strain).

164 Four FRC mixtures were prepared, always using 0.5 % of fibres in volume
165 of matrix, and also combining the aforementioned ISFs and RSFs:

- 166 • RSFRC 0-05: with only ISFs (RSFs=0%).
- 167 • RSFRC 25-05: with 25% of ISFs replaced by an equal amount of RSFs.
- 168 • RSFRC 50-05: with 50% of ISFs replaced by an equal amount of RSFs.
- 169 • RSFRC 100-05: with all RSFs.

170 3.2. Methods

171 The concrete mixtures described in the previous section were prepared
172 by using a laboratory mixer. Both coarse and fine aggregates were saturated
173 and mixed; subsequently, cement, fibres and, finally, a super-plasticizer were
174 added. The REF mixture, whose composition is described in Table 1, was
175 designed for a target slump value of 150-180 mm; a value of 175 mm was actu-
176 ally measured at fresh state. Moreover, the cementitious matrix composition
177 of all FRC specimens was kept fairly unchanged; only the super-plasticizer
178 was slightly adjusted for controlling the influence of fibres on the resulting
179 workability.

180 Three cube samples of $150 \times 150 \times 150$ mm³ and beam specimens of
181 $150 \times 150 \times 600$ mm³ (Fig. 10) were cast in polyurethane moulds and duly
182 vibrated. One of the cubic samples (labelled as “white”) was extracted from
183 each mixture before fibre mixing: it was tested in compression and compared
184 with the corresponding FRC samples with the aim to observe the actual
185 contribution of fibres on the compressive strength in each different mixture.

186 After 36 h the concrete samples were removed from the moulds. Then, the
187 hardened samples were notched (through a 2.0 mm wide-slit) of 45 mm depth
188 and starting from the bottom surface of the sample (Fig. 11b). Moreover,
189 all concrete specimens were cured in a water bath (100 % humidity) at a
190 constant temperature of 22°C, up to reach the 28 days of curing. All the
191 aforementioned preparation procedures were carried out according to UNI-
192 11039-2 [27].

193 Table 3 outlines the experimental programme reported in this paper. Ex-
194 perimental tests were carried out according to the procedures described in the
195 UNI-11039-2 [27]. Four-point bending tests of notched beams, as shown in
196 Fig. 11(a), were performed in displacement control (having displacement rate
197 of 0.005 mm/sec). Relevant load and displacement quantities were measured
198 and recorded during all tests. Particularly, the crack-tip opening displace-
199 ment were measured by means of dedicated transducers which monitored
200 the relative displacements of the two sides of the notch tip (Fig. 12). Fur-
201 thermore, compressive tests were performed according to EN-12390-3 [32]
202 for measuring the cubic compressive strength of the SFRCs at the time of
203 testing.

204 4. Experimental results

205 4.1. Compression tests

206 The results of compression tests are summarised in Table 4 reporting the
207 average values of compressive strengths obtained from cubic samples of the
208 plain concrete and FRC mixtures considered in this study. The same table
209 also reports the average values of specific weight measured in hardened sam-
210 ples of the same concrete mixtures. As widely documented in the scientific
211 literature [30], no significant difference was observed in terms of compressive
212 strengths of both the so-called “white” and SFRC specimens.

213 This means that, at least for the volume fraction considered in this study,
214 the resulting compressive strength of FRC is mainly controlled by the matrix
215 properties. Conversely, fibres only play a role in the post-cracking regime.
216 The observed σ - ϵ curves are omitted herein for the sake of brevity and the
217 influence of fibres on the post-cracking response of FRC is discussed into
218 details for the case of bending tests.

219 *4.2. Four-point bending tests*

220 Four-point bending tests were performed with the aim of characterising
221 the post-cracking flexural behaviour of HIRSFRC samples (Fig. 13): UNI-
222 11039-1 [26] and UNI-11039-2 [27] provisions were taken into account for this
223 purpose.

224 Figs. 14a-14d report the experimental curves of the vertical load, P , ver-
225 sus the corresponding Crack Tip Opening Displacement ($CTOD_m$) curves,
226 obtained in the tests: $CTOD_m$ represents the mean of the two opposite
227 $CTOD_s$.

228 Based on the experimental evidence, the post-cracking response in bend-
229 ing of FRC specimens reinforced with only ISFs was characterised by a sig-
230 nificant post-cracking toughness (Fig. 14a), which is due to the bridging
231 action of fibres and cannot be obtained in plain concrete [30].

232 The effect of replacing increasing amount of ISFs with an equal quantity
233 of RSFs can be easily understood by analysing the curves depicted in Figs.
234 14a-14d. The post-cracking behaviour of FRC is generally characterised by
235 a more pronounced softening range in specimens characterised by a greater
236 quantity of RSFs in substitution of ISFs. This is a result of the lower effi-
237 ciency of the recycled fibres with respect to the industrial ones, which are
238 specifically designed to exhibit a good interaction with the concrete ma-
239 trix. Particularly, recycled fibres are not straight, have no hooks and have
240 (generally) lower aspect ratios: these are the main reasons explaining the
241 (expected) decay resulting from replacing part (to total) of industrial with
242 an equal amount (in weight) of recycled fibres.

243 The steeper slope of the post-peak response observed for RSFRC 25-05
244 (Fig. 14b) is clearly due to the fact that the recycled fibres employed in
245 those specimens need a wider crack opening for mobilising their bridging
246 effect. The post-peak slope is even steeper for RSFRC 50-05 (Fig. 14c) and
247 RSFRC 100-05 (Fig. 14d) where the actual volume fraction of RSF is even
248 higher.

249 Nevertheless, a significant increase in toughness can be observed for all
250 FRC specimens with respect to the significantly brittle behaviour character-
251 ising the post-cracking response of plain concrete.

252 Finally, it is worth highlighting that a fairly uniform distribution of fibres
253 throughout the cracked surface was observed in all tested specimens: Fig. 15
254 shows the fracture surface obtained for one of the specimen made of RSFRC
255 100-05.

256 **5. Analysis of results**

257 Three representative parameters, defined in [UNI-11039-2](#) [27], can be eval-
 258 uated and compared for the FRC mixtures under investigation, with the aim
 259 of identifying and describing their post-cracking response: they are defined as
 260 the first crack strength (f_{lf}) and two equivalent post-cracking strengths: the
 261 first flexural strength ($f_{eq(0-0.6)}$) corresponds to a *CTOD* ranging between
 262 $CTOD_0$ and $CTOD_0 + 0.6$ mm and is supposed to be relevant significant for
 263 the Serviceability Limit State; the second one ($f_{eq(0.6-3.0)}$) refers to a *CTOD*
 264 ranging between $CTOD_0 + 0.6$ and $CTOD_0 + 3$ mm which is rather relevant
 265 for the Ultimate Limit State [33].

266 According to [UNI-11039-2](#) [27], the first crack strength values, f_{lf} , defin-
 267 ing the post-cracking response of HIRSFRC, was evaluated in each sample
 268 as

$$f_{lf} = \frac{P_{lf} \cdot l}{b(h - a_0)^2} \quad (1)$$

269 where P_{lf} represents the first crack load [N], b , h and l are the width [mm],
 270 height [mm] and length [mm] of the beam, respectively, and a_0 [mm] repre-
 271 sents the notch depth.

272 Fig. 16 shows the comparisons of the mean values of first crack strength
 273 and the two equivalent crack resistances, defined in standard *CTOD_m* ranges,
 274 i.e. [$CTOD_{m_0}; CTOD_{m_0} + 0.6$ mm] and [$CTOD_{m_0} + 0.6; CTOD_{m_0} + 3.0$ mm].
 275 $CTOD_{m_0}$ is the Crack Tip Opening Displacement (mean value) correspond-
 276 ing to the peak load of the reference specimen.

277 The following quantities, known as “equivalent crack resistances” $f_{eq(0-0.6)}$
 278 and $f_{eq(0.6-3.0)}$, are defined as follows

$$f_{eq(0-0.6)} = \frac{l}{b(h-a_0)^2} \frac{U_1}{0.6} \quad (2)$$

$$f_{eq(0.6-3.0)} = \frac{l}{b(h-a_0)^2} \frac{U_2}{2.4}$$

279 being U_1 and U_2 work capacity measures derived by means of the following
 280 relations

$$U_1 = \int_{CTOD_{m_0}}^{CTOD_{m_0}+0.6} P(CTOD_m) dCTOD_m \quad (3)$$

$$U_2 = \int_{CTOD_{m_0}+0.6}^{CTOD_{m_0}+3.0} P(CTOD_m) dCTOD_m$$

281 calculated on the HIRSFRC test data.

282 As a matter of principle, the quantities described by Eq. (3) represent the
283 enclosed area (toughness measure) under the $P-CTOD_m$ curves between the
284 range $[CTOD_{m_0}; CTOD_{m_0} + 0.6 \text{ mm}]$ and $[CTOD_{m_0} + 0.6; CTOD_{m_0} + 3.0 \text{ mm}]$
285 for U_1 and U_2 , respectively. Fig. 17 shows such energy absorption values of
286 each sample and calculated by means of the Eq. (3). Keeping in mind the me-
287 chanical meaning of those parameters, these results show that, **as expected**,
288 all specimens, reinforced with a total amount of 40 kg/m^3 of steel **fibres**
289 (equivalent to 0.5 % in **fibre** volume fraction), mainly exhibit a softening
290 behaviour in the post-cracking regime.

291 Moreover, ductility indices can be considered as further objective “mea-
292 sures” of the **fibre** bridging mechanisms and the following ductility measures
293 were calculated [27]

$$D_0 = f_{eq(0-0.6)} / f_{lf} \quad (4)$$

294 and

$$D_1 = f_{eq(0.6-3.0)} / f_{eq(0-0.6)}. \quad (5)$$

295 Fig. 18 reports the values of ductility indices (defined by Eqs. (4) and
296 (5)) for the various tested beams. According to the classification of the UNI-
297 11039-1 [26], all the cementitious composites, tested in this experimental
298 campaign, can be classified as “crack-softening” media, as both D_0 and D_1
299 < 1 .

300 Finally, it is worth highlighting that UNI-11039-1 [26] states that the
301 D_0 index should not be lower than 0.5 for a FRC to be used in structural
302 applications. Based on this criterion, Fig. 18 shows that all SFRC mixtures,
303 even the one reinforced with only RSFs, can be considered as a structural
304 **fibre** reinforced cementitious material.

305 6. Conclusions

306 This experimental research was intended at investigating the mechanical
307 behaviour of concrete reinforced with both recycled and industrial steel **fibres**.
308 Based on the obtained results the following observations can be highlighted:

- 309 • as expected, the observed compressive strength is almost unaffected by
310 the presence of **fibres** and, then, no significant difference was detected
311 between the FRC specimens with only industrial **fibres** and **the ones**
312 **made with an increasing proportion of recycled fibres**;

- 313 • on the contrary, as it was also expected, the bending behaviour ob-
314 served in the experimental tests was significantly influenced by the
315 **fibre** contribution;
- 316 • in this regard, a significant decay in the post-peak cracking behaviour
317 was observed as a result of the partial to total replacement of industrial
318 **fibres** with an equal amount of recycled ones;
- 319 • particularly, the higher is the amount of recycled **fibres**, the more sig-
320 nificant is the reduction the post-cracking toughness (in terms of equiv-
321 alent post-cracking strengths and/or ductility indices) observed in the
322 four-point bending tests;
- 323 • nevertheless, it is worth highlighting that, in spite of the low amount of
324 **fibres** (0.5 % in volume), a significant increase in the equivalent fracture
325 energy was observed for FRC specimens with respect to the reference
326 (“white”) ones, even in the case of a total replacement of ISFs with
327 RSFs.

328 Finally, the presented results confirmed the promising application of con-
329 crete reinforced with recycled steel **fibres** derived from waste tyres. However,
330 the proposed results clearly demonstrate that industrial **fibres** cannot be
331 replaced by an equal amount of (unprocessed) recycled ones without a sig-
332 nificant decay in the relevant mechanical properties. In fact, the definition
333 of an “equivalent” (and higher) amount of recycled **fibres** which might be
334 substituted to a certain amount of industrial ones without significant loss
335 in terms of mechanical properties is a further possible prospect for the use
336 of HIRSFRCs in structural applications. However, further investigations are
337 still necessary to completely understand this and the other relevant aspects
338 of the mechanical response of these materials.

339 **Acknowledgement**

340 The authors are grateful to “Calcestruzzi Irpini S.p.A” and “General
341 Admixtures S.p.A.” for their important support to the experimental inves-
342 tigation. “RPN Tyres S.r.l” is also acknowledged for having supplied the
343 recycled steel **fibres** for the experimental campaign.

344 Finally, it has to be outlined that this study is part of the activities carried
345 out by the authors within the “EnCoRe” project (www.encore-fp7.unisa.it),

346 funded by the European Union within the Seventh Framework Programme
347 (FP7-PEOPLE-2011-IRSES, n. 295283).

348 **References**

- 349 [1] Tchobanoglous, G., Kreith, F.. Handbook of solid waste management.
350 McGraw-Hill New York; 2002.
- 351 [2] Sienkiewicz, M., Kucinska-Lipka, J., Janik, H., Balas, A.. Progress
352 in used tyres management in the European Union: A review. Waste
353 Management 2012;32(10):1742 – 1751.
- 354 [3] EU-Directive, . 1999/31/EC of the Council of 26 April 1999 on the
355 landfill of waste. Off. J. Eur. Union, L182, 1-19; 1999.
- 356 [4] Sharma, V., Fortuna, F., Mincarini, M., Berillo, M., Cornacchia,
357 G.. Disposal of waste tyres for energy recovery and safe environment.
358 Applied Energy 2000;65(1):381 – 394.
- 359 [5] Ganjian, E., Khorami, M., Maghsoudi, A.A.. Scrap-tyre-rubber re-
360 placement for aggregate and filler in concrete. Construction and Building
361 Materials 2009;23(5):1828 – 1836.
- 362 [6] Centonze, G., Leone, M., Aiello, M.. Steel fibers from waste tires as
363 reinforcement in concrete: A mechanical characterization. Construction
364 and Building Materials 2012;36(0):46 – 57.
- 365 [7] Graeff, A.G., Pilakoutas, K., Neocleous, K., Peres, M.V.N.. Fa-
366 tigue resistance and cracking mechanism of concrete pavements rein-
367 forced with recycled steel fibres recovered from post-consumer tyres.
368 Engineering Structures 2012;45(0):385 – 395.
- 369 [8] Yung, W.H., Yung, L.C., Hua, L.H.. A study of the durability proper-
370 ties of waste tire rubber applied to self-compacting concrete. Construc-
371 tion and Building Materials 2013;41(0):665 – 672.
- 372 [9] Naaman, A., Reinhardt, H.. Proposed classification of HPFRC
373 composites based on their tensile response. Materials and Structures
374 2006;39:547–555.

- 375 [10] Qian, X., Zhou, X., Mu, B., Li, Z.. Fiber alignment and property
376 direction dependency of FRC extrudate. *Cement and Concrete Research*
377 2003;33(10):1575 – 1581.
- 378 [11] ACI-544.1-96, . State-of-the-Art Report on Fiber Reinforced Concrete.
379 Reported by ACI Committee 544, American Concrete Institute. 1996.
- 380 [12] Bartl, A., Hackl, A., Mihalyi, B., Wistuba, M., Marini, I.. Recy-
381 cling of fibre materials. *Process Safety and Environmental Protection*
382 2005;83(B4):351 – 358.
- 383 [13] Tlemat, H., Pilakoutas, K., Neocleous, K.. Stress-strain characteristic
384 of SFRC using recycled fibres. *Materials and structures* 2006;39(3):365–
385 377.
- 386 [14] Neocleous, K., Tlemat, H., Pilakoutas, K.. Design issues for concrete
387 reinforced with steel fibers, including fibers recovered from used tires.
388 *Journal of materials in civil engineering* 2006;18(5):677 – 685.
- 389 [15] Aiello, M.A., Leuzzi, F., Centonze, G., Maffezzoli, A.. Use of steel
390 fibres recovered from waste tyres as reinforcement in concrete: Pull-
391 out behaviour, compressive and flexural strength. *Waste management*
392 2009;29(6):1960 – 1970.
- 393 [16] Sorelli, L., Meda, A., Plizzari, G.. Bending and uni-axial tensile
394 tests on concrete reinforced with hybrid steel fibers. *ASCE - Journal of*
395 *Materials in Civil Engineering* 2005;17(5):519 – 527.
- 396 [17] Park, S., Kim, D., Ryu, G., Koh, K.. Tensile behavior of ultra high
397 performance hybrid fiber reinforced concrete. *Cement and Concrete*
398 *Composites* 2012;34(2):172 – 184.
- 399 [18] Hsie, M., Tu, C., Song, P.. Mechanical properties of polypropylene
400 hybrid fiber-reinforced concrete. *Materials Science and Engineering: A*
401 2008;494(1–2):153 – 157.
- 402 [19] Kim, D., Park, S., Ryu, G., Koh, K.. Comparative flexural behavior
403 of hybrid ultra high performance fiber reinforced concrete with different
404 macro fibers. *Construction and Building Materials* 2011;25(11):4144 –
405 4155.

- 406 [20] Yao, W., Li, J., Wu, K.. Mechanical properties of hybrid fiber-
407 reinforced concrete at low fiber volume fraction. *Cement and Concrete*
408 *Research* 2003;33(1):27 – 30.
- 409 [21] Dawood, E., Ramli, M.. Mechanical properties of high strength flow-
410 ing concrete with hybrid fibers. *Construction and Building Materials*
411 2012;28(1):193 – 200.
- 412 [22] Libre, N., Shekarchi, M., Mahoutian, M., Soroushian, P.. Me-
413 chanical properties of hybrid fiber reinforced lightweight aggregate con-
414 crete made with natural pumice. *Construction and Building Materials*
415 2011;25(5):2458 – 2464.
- 416 [23] Sahmaran, M., Yaman, I.. Hybrid fiber reinforced self-compacting
417 concrete with a high-volume coarse fly ash. *Construction and Building*
418 *Materials* 2007;21(1):150 – 156.
- 419 [24] Ding, Y., Azevedo, C., Aguiar, J., Jalali, S.. Study on residual
420 behaviour and flexural toughness of fibre cocktail reinforced self com-
421 pacting high performance concrete after exposure to high temperature.
422 *Construction and Building Materials* 2012;26(1):21 – 31.
- 423 [25] Akcay, B., Tasdemir, M.. Mechanical behaviour and fibre dispersion
424 of hybrid steel fibre reinforced self-compacting concrete. *Construction*
425 *and Building Materials* 2012;28(1):287 – 293.
- 426 [26] UNI-11039-1, . Steel fibre reinforced concrete - Definitions, classification
427 and designation. UNI Editions, Milan, Italy; 2003.
- 428 [27] UNI-11039-2, . Steel fibre reinforced concrete - Test method to determine
429 the first crack strength and ductility indexes. UNI Editions, Milan, Italy;
430 2003.
- 431 [28] CNR-204/2006, . CNR – Consiglio Nazionale delle Ricerche: Istruzioni
432 per la progettazione, l'esecuzione ed il controllo di strutture di calces-
433 truzzo fibrorinforzato [in Italian]. 2006.
- 434 [29] UNI-EN-12620, . Aggregates for concrete, volume Ref. No. EN
435 12620:2002 E. Europ. Committee for Standardization, Brussels; 2002.

- 436 [30] Caggiano, A., Cremona, M., Faella, C., Lima, C., Martinelli, E..
437 Fracture behavior of concrete beams reinforced with mixed long/short
438 steel fibers. *Construction and Building Materials* 2012;37(0):832 – 840.
- 439 [31] Officine-Maccaferri, . Cold drawn steel wire fibre, for concrete reinforce-
440 ment. TECHNICAL DATA SHEET, WIRAND FIBRE FS7; 2010.
- 441 [32] EN-12390-3, . Testing hardened concrete. Part 3: compressive strength
442 of test specimens. BSI; 2009.
- 443 [33] di Prisco, M., Plizzari, G., Vandewalle, L.. Fibre reinforced concrete:
444 new design perspectives. *Material Structures* 2009;42(9):1261 – 1281.

445 **List of Figures**

446 Figure 1 Recycled steel fibres employed for the HIRSFRC. 19
447 Figure 2 SEM analysis of RSF. 20
448 Figure 3 Frequency of diameter measurements. 20
449 Figure 4 Frequency of fibre length measurements. 21
450 Figure 5 Frequency of measured fibre developed lengths. 21
451 Figure 6 Frequency of l_f/l_d ratio. 22
452 Figure 7 Frequency of the aspect ratio. 22
453 Figure 8 Grain size distribution of the “REF” mixture. 23
454 Figure 9 Industrial fibre types FS7 [31] employed for the HIRSFRC. 23
455 Figure 10 Geometry of the notched beam in four-point bending. . . . 24
456 Figure 11 Four-point bending test: (a) experimental set-up and (b)
457 the vertical notch at the bottom surface of the specimen. 24
458 Figure 12 Disposition of the instrumentation for the four-point bend-
459 ing tests. 25
460 Figure 13 Cracked configuration after the 4PB test of HIRSFRC
461 notched beams. 25
462 Figure 14 Vertical force - $CTOD_m$ curves. 26
463 Figure 15 Observed distribution of fibres at crack section for one of
464 the specimens (mixture RSFRC 100-05). 26
465 Figure 16 Comparisons between the first crack strength, f_{lf} , with
466 the equivalent crack resistances, $f_{eq(0-0.6)}$ and $f_{eq(0.6-3.0)}$
467 [27]. The vertical segments represent the range between
468 the minimum and the maximum value. 27
469 Figure 17 Energy absorption measures U_1 and U_2 according to UNI-
470 11039-2 [27]. The vertical segments represent the range
471 between the minimum and the maximum value. 27
472 Figure 18 Indices of the ductility according to UNI-11039-2 [27]. The
473 vertical segments represent the range between the mini-
474 mum and the maximum value. 27

475 **List of Tables**

476 Table 1 Mixture design per cubic meter of the reference concrete. . . 17
477 Table 2 Specific weight and absorption of aggregates and sand. . . . 17
478 Table 3 Considered mixture types of the experimental programme. . . 18

479
480

Table 4 Densities and cube compressive strengths measured in each mixture. 18

Table 1: Mixture design per cubic meter of the reference concrete.

Material	Dosage [kg/m ³]
Sand	1012
Coarse agg. N1	134
Coarse agg. N2	764
Cement 42.5R	320
Free water	163
Water absorption	17
Superplasticizer	2.75

Table 2: Specific weight and absorption of aggregates and sand.

Material	Specific Weight [kg/m ³]	Absorption
Sand	2690	1.20%
Coarse agg. N1	2690	0.70%
Coarse agg. N2	2690	0.50%

Table 3: Considered mixture types of the experimental programme.

Mixtures	Compression tests (28 days)	Four-Point Bending Beams (28 days)
“REF”	3	3
RSFRC 0-05	3	3
RSFRC 25-05	3	3
RSFRC 50-05	3	3
RSFRC 100-05	3	3

Table 4: Densities and cube compressive strengths measured in each mixture.

Mixture Label	Specific weight [kg/m ³]		f _{c,cube} at 28 days [Mpa]	
	white	SFRC	white	SFRC (mean of two)
REF	2371		42.59 (mean of three)	
RSFRC 0-05	2376	2413	40.57	39.01
RSFRC 25-05	2428	2435	36.42	36.52
RSFRC 50-05	2459	2450	36.89	36.74
RSFRC 100-05	2446	2491	36.69	37.37



Figure 1: Recycled steel fibres employed for the HIRSFRC.

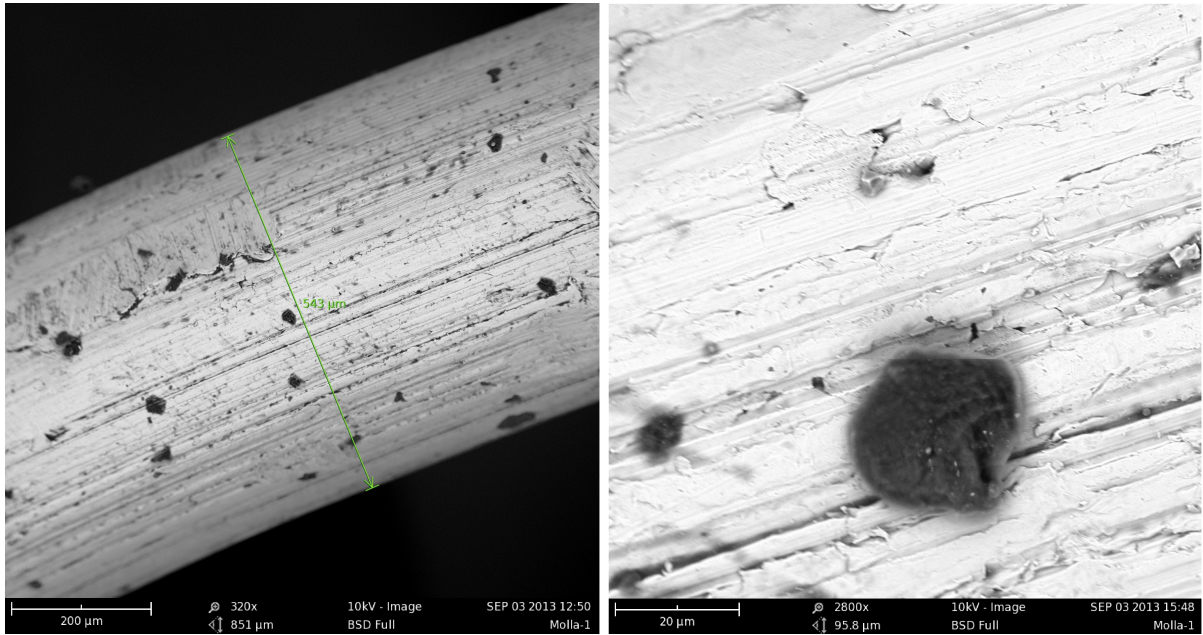


Figure 2: SEM analysis of RSF.

diameters.pdf

Figure 3: Frequency of diameter measurements.

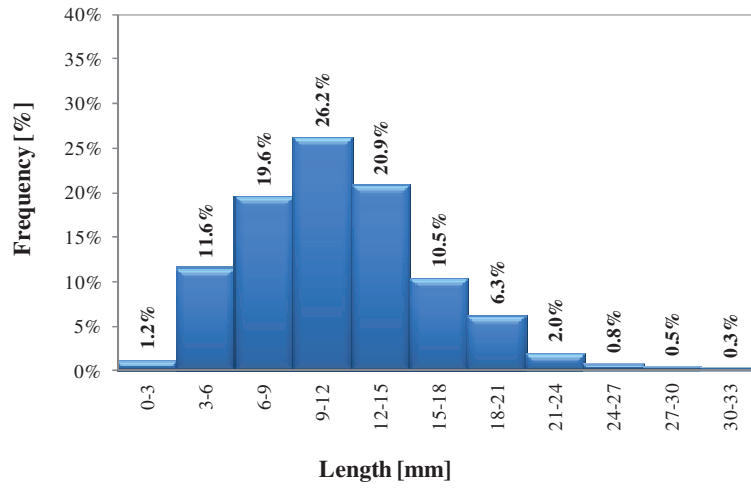


Figure 4: Frequency of fibre length measurements.

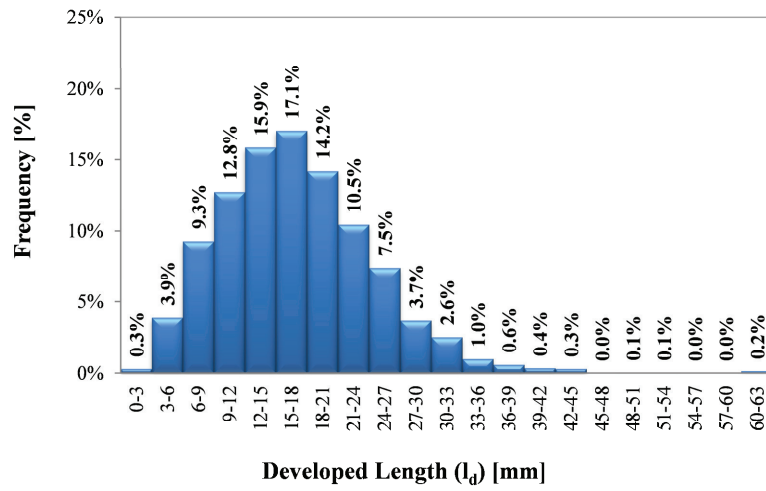


Figure 5: Frequency of measured fibre developed lengths.

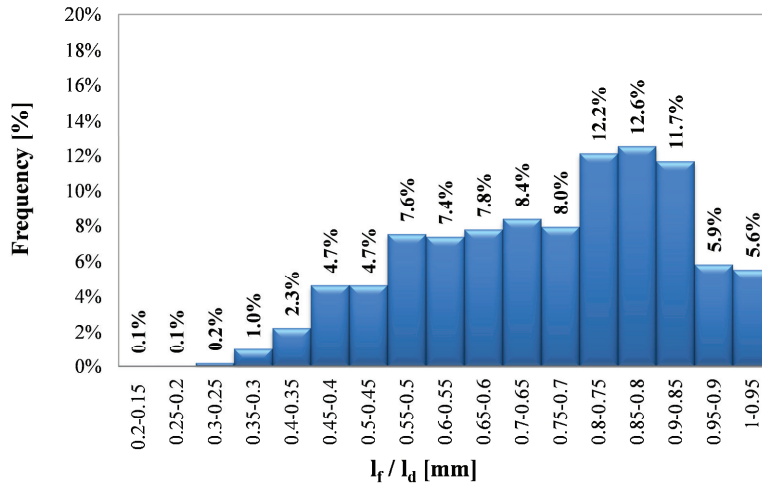


Figure 6: Frequency of l_f / l_d ratio.

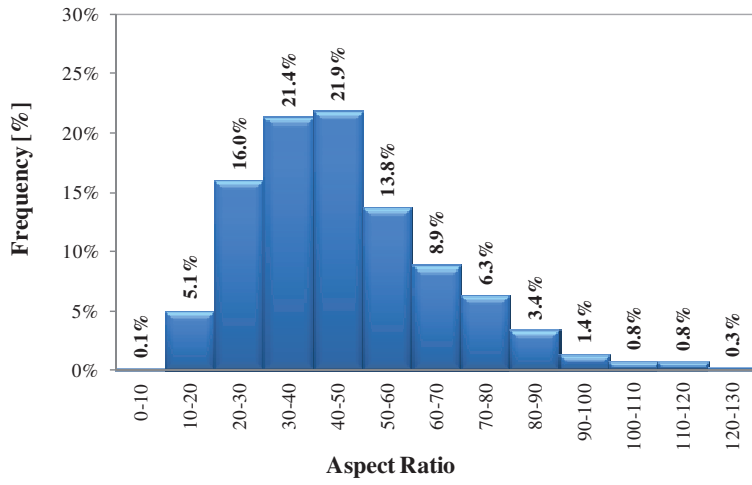


Figure 7: Frequency of the aspect ratio.

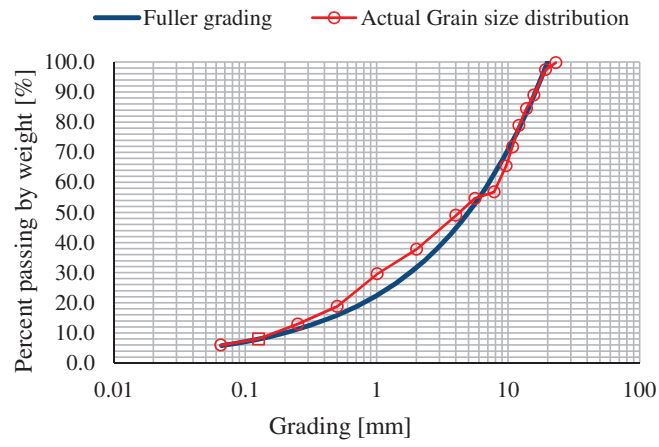


Figure 8: Grain size distribution of the “REF” mixture.



Figure 9: Industrial fibre types FS7 [31] employed for the HIRSFRC.

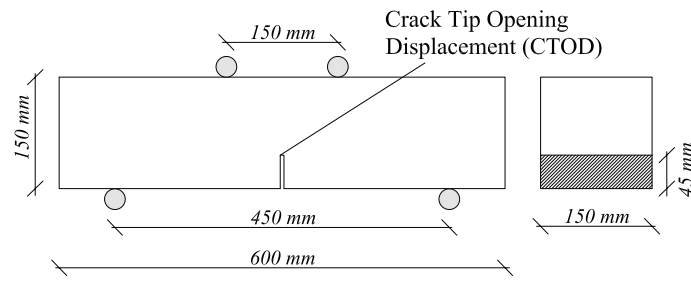


Figure 10: Geometry of the notched beam in four-point bending.

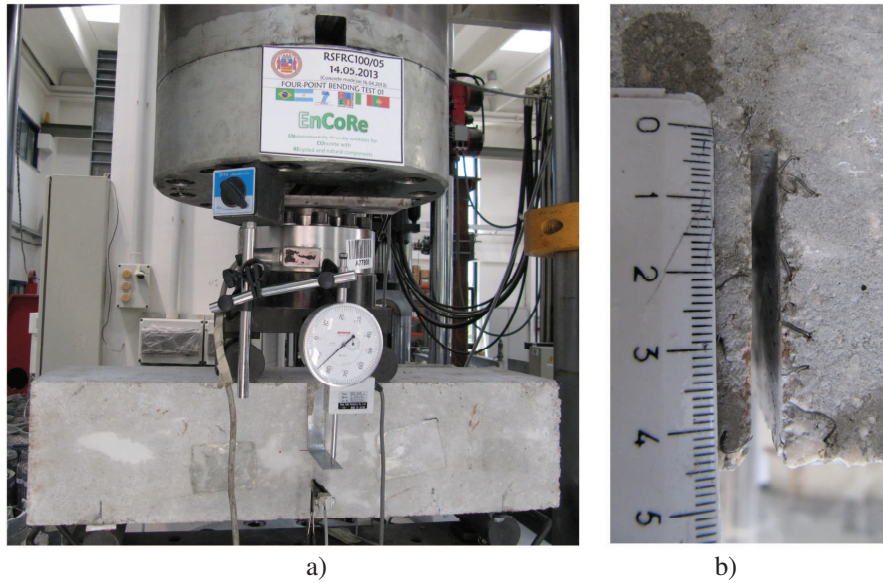


Figure 11: Four-point bending test: (a) experimental set-up and (b) the vertical notch at the bottom surface of the specimen.



Figure 12: Disposition of the instrumentation for the four-point bending tests.



Figure 13: Cracked configuration after the 4PB test of HIRSFRC notched beams.

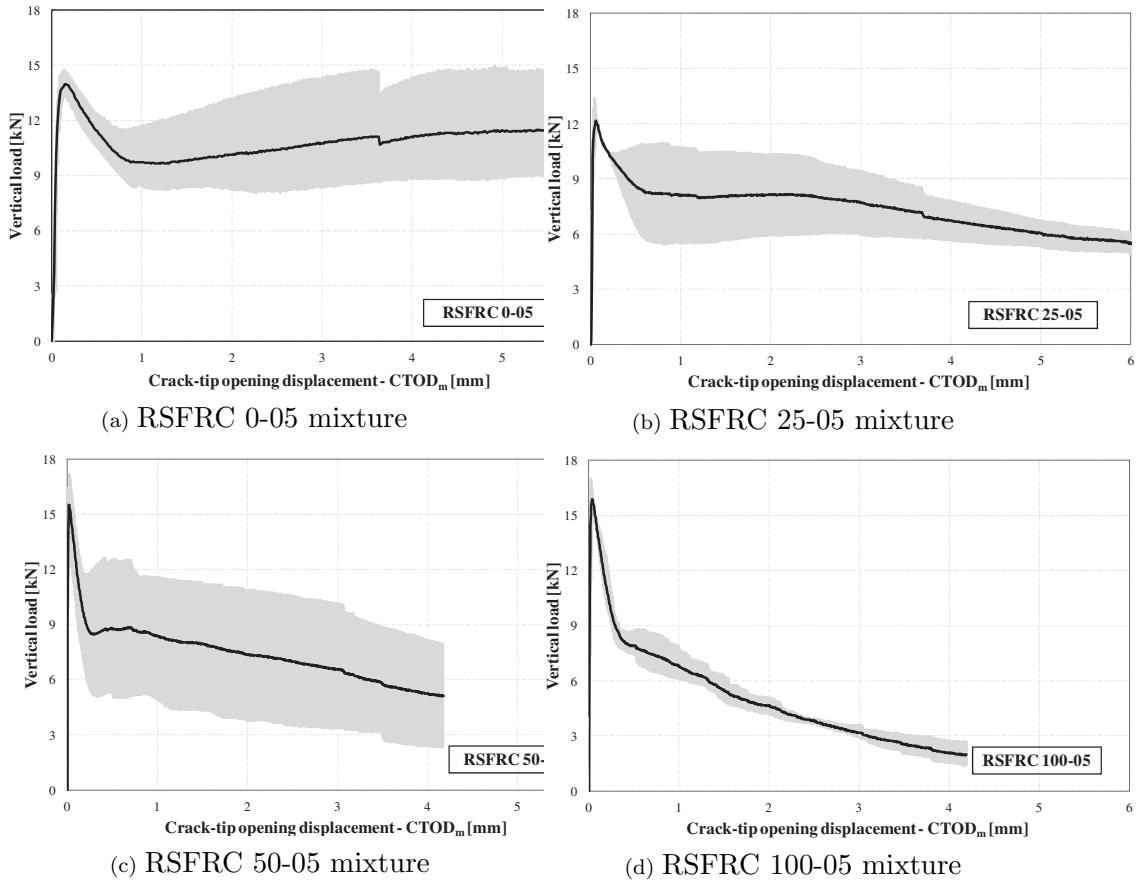


Figure 14: Vertical force - $CTOD_m$ curves.

cross_section.jpg

Figure 15: Observed distribution of fibres at crack section for one of the specimens (mixture RSFRC 100-05).

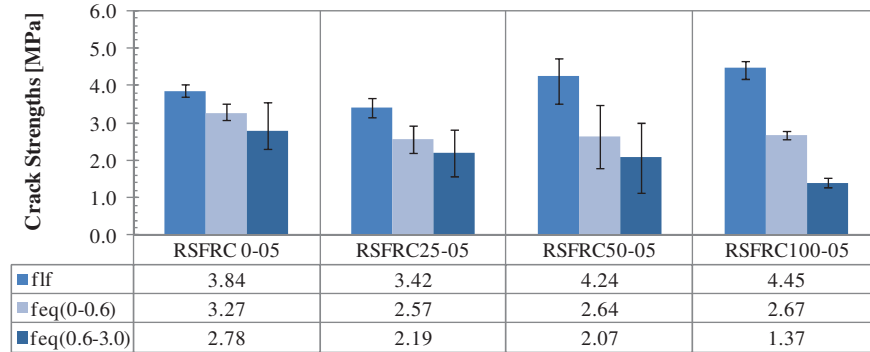


Figure 16: Comparisons between the first crack strength, f_{lf} , with the equivalent crack resistances, $f_{eq(0-0.6)}$ and $f_{eq(0.6-3.0)}$ [27]. The vertical segments represent the range between the minimum and the maximum value.

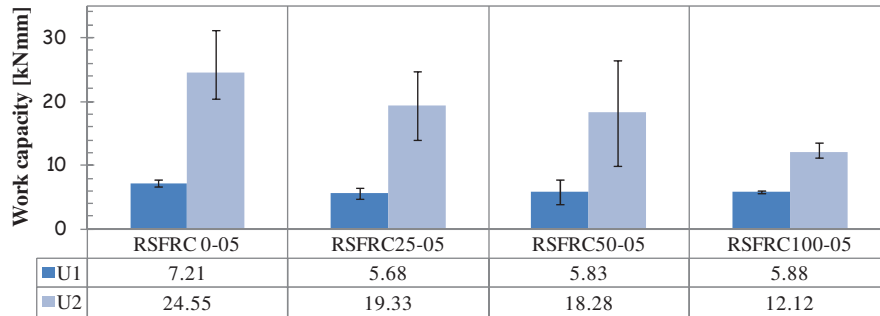


Figure 17: Energy absorption measures U_1 and U_2 according to UNI-11039-2 [27]. The vertical segments represent the range between the minimum and the maximum value.

DOD1.pdf

Figure 18: Indices of the ductility according to UNI-11039-2 [27]. The vertical segments represent the range between the minimum and the maximum value.